

# Implication of Formation Mechanisms of HC<sub>5</sub>N in TMC-1 as Studied by <sup>13</sup>C Isotopic Fractionation

Kotomi Taniguchi<sup>1,2</sup>, Hiroyuki Ozeki<sup>1</sup>, Masao Saito<sup>2,3</sup>, Nami Sakai<sup>4,5</sup>, Fumitaka  
Nakamura<sup>2,6</sup>, Seiji Kamenno<sup>2,7</sup>, Shuro Takano<sup>2,3,8</sup>, and Satoshi Yamamoto<sup>4</sup>

kotomi.taniguchi@nao.ac.jp

Received \_\_\_\_\_; accepted \_\_\_\_\_

2015 November 26 version

---

<sup>1</sup>Department of Environmental Science, Faculty of Science, Toho University, Miyama, Funabashi, Chiba 274-8510, Japan

<sup>2</sup>Department of Astronomical Science, School of Physical Science, SOKENDAI (The Graduate University for Advanced Studies), Osawa, Mitaka, Tokyo 181-8588, Japan

<sup>3</sup>Nobeyama Radio Observatory, National Astronomical Observatory of Japan, Minamimaki, Minamisaku, Nagano 384-1305, Japan

<sup>4</sup>Department of Physics, Faculty of Science, The University of Tokyo, Hongo, Bunkyo, Tokyo 113-0033, Japan

<sup>5</sup>The Institute of Physical and Chemical Research (RIKEN), Wako, Saitama 351-0198, Japan

<sup>6</sup>National Astronomical Observatory of Japan, Osawa, Mitaka, Tokyo 181-8588, Japan

<sup>7</sup>Joint ALMA Observatory, Alonso de Cordova 3107 Vitacura, Santiago 763 0355, Chile

<sup>8</sup>Department of Physics, General Studies, College of Engineering, Nihon University, Koriyama, Fukushima 963-8642, Japan

## ABSTRACT

We observed the  $J = 9 - 8$  and  $16 - 15$  rotational transitions of the normal species and five  $^{13}\text{C}$  isotopologues of  $\text{HC}_5\text{N}$  to study its formation mechanisms toward the cyanopolyne peak in Taurus Molecular Cloud-1, with the 45-m radio telescope of Nobeyama Radio Observatory. We detected the five  $^{13}\text{C}$  isotopologues with high signal-to-noise ratios between 12 and 20, as well as the normal species. The abundance ratios of the five  $^{13}\text{C}$  isotopologues of  $\text{HC}_5\text{N}$  are found to be  $1.00 : 0.97 : 1.03 : 1.05 : 1.16 (\pm 0.19) (1\sigma)$  for  $[\text{H}^{13}\text{CCCCCN}] : [\text{HC}^{13}\text{CCCCN}] : [\text{HCC}^{13}\text{CCCN}] : [\text{HCCC}^{13}\text{CCN}] : [\text{HCCCC}^{13}\text{CN}]$ . We do not find any significant differences among the five  $^{13}\text{C}$  isotopologues. The averaged  $[\text{HC}_5\text{N}]/[^{13}\text{C isotopologues}]$  abundance ratio is determined to be  $94 \pm 6 (1\sigma)$ , which is slightly higher than the local interstellar elemental  $^{12}\text{C}/^{13}\text{C}$  ratio of  $60 - 70$ . Possible formation pathways are discussed on the basis of these results.

*Subject headings:* astrochemistry — ISM: individual objects(TMC-1) — ISM: molecules

## 1. Introduction

More than 180 molecules have been detected in the interstellar medium and circumstellar shells of evolved stars, and approximately 40% of them are classified into carbon-chain molecules. It is therefore of fundamental importance for astrochemistry to study their formation processes. However, these molecules are so reactive due to unsaturated chemical bonds and/or unpaired electrons that laboratory measurements of their reaction rates are not routine experiments. Although formation mechanisms of the carbon-chain molecules have mainly been studied by chemical model calculations (e.g. McElroy et al. 2013; Wakelam et al. 2015), it is still difficult to reproduce molecular abundances derived by observations, and to determine formation mechanisms of carbon-chain molecules, because of uncertain rate coefficients and of poor knowledge of elementary reactions involving carbon-chain molecules.

Another method to study major formation pathways of molecules is based mainly on observations. Recent developments of radio astronomical instruments allow us to detect low-abundance species, including rare isotopologues, with a reasonable observation time. Formation mechanisms of some representative carbon-chain molecules have been investigated by observing their  $^{13}\text{C}$  isotopic fractionation, such as  $\text{HC}_3\text{N}$  (Takano et al. 1998),  $\text{CCH}$  (Sakai et al. 2010),  $\text{CCS}$  (Sakai et al. 2007),  $\text{C}_3\text{S}$ , and  $\text{C}_4\text{H}$  (Sakai et al. 2013), toward the cyanopolyne peak in Taurus Molecular Cloud-1 (TMC-1 CP;  $d = 140$  pc), and *cyclic*- $\text{C}_3\text{H}_2$  (Yoshida et al. 2015) toward the low-mass star-forming region L1527. TMC-1 CP is a representative cold dark cloud where various carbon-chain molecules are abundant. For instance, Kaifu et al. (2004) carried out spectral line survey observations in the 8.8 – 50 GHz region toward TMC-1 CP with the 45-m radio telescope of Nobeyama Radio Observatory (NRO), and demonstrated that this source is rich in carbon-chain molecules.

Cyanoacetylene,  $\text{HC}_3\text{N}$ , is a very abundant carbon-chain molecule in TMC-1 CP. Takano et al. (1998) observed three  $^{13}\text{C}$  isotopologues of  $\text{HC}_3\text{N}$  toward TMC-1 CP, and the relative abundance of  $\text{HCC}^{13}\text{CN}$  is significantly higher than that of the other isotopologues:  $[\text{H}^{13}\text{CCCN}] : [\text{HC}^{13}\text{CCN}] : [\text{HCC}^{13}\text{CN}]$  is 1.0 : 1.0 : 1.4. These results imply that  $\text{HC}_3\text{N}$  is mainly formed by the reaction between a hydrocarbon molecule with two equivalent carbon atoms and a molecule with one carbon atom, whose  $^{12}\text{C}/^{13}\text{C}$  ratios are different from each other. According to *ab initio* calculations, the reaction of  $\text{C}_2\text{H}_2 + \text{CN}$  is exothermic, and has no significant energy barrier (Woon & Herbst 1997; Fukuzawa et al. 1998). The laboratory experiments show that the rate coefficient for this reaction is sufficiently large ( $k \geq 4 \times 10^{-10} \text{ cm}^3 \text{ molecule}^{-1} \text{ s}^{-1}$ ) at low temperatures (Sims et al. 1993). Considering these results, Takano et al. (1998) suggested that  $\text{HC}_3\text{N}$  is formed by the reaction between  $\text{C}_2\text{H}_2$  and  $\text{CN}$ .

It can naturally be predicted that  $\text{HC}_5\text{N}$  is formed by the similar mechanism of  $\text{HC}_3\text{N}$ , the reaction of  $\text{C}_4\text{H}_2 + \text{CN}$ . Fukuzawa et al. (1998) conducted *ab initio* calculations on the reactions of  $\text{C}_{2n}\text{H}_2 + \text{CN}$  ( $n = 1 - 4$ ), which form  $\text{HC}_{2n+1}\text{N}$ , and found that these reactions are all exothermic and have no energy barriers. In addition, Seki et al. (1996) measured the rate constant for the reaction  $\text{C}_4\text{H}_2 + \text{CN}$  to be  $(4.2 \pm 0.2) \times 10^{-10} \text{ cm}^3 \text{ molecule}^{-1} \text{ s}^{-1}$  at the room temperature. These results suggest that  $\text{HC}_5\text{N}$  can be formed by the reaction of  $\text{C}_4\text{H}_2 + \text{CN}$ . If so, we would be able to observe different abundances of the five  $^{13}\text{C}$  isotopologues of  $\text{HC}_5\text{N}$ .

Observations of the  $^{13}\text{C}$  isotopologues of  $\text{HC}_5\text{N}$  were carried out toward TMC-1 CP by Takano et al. (1990). Although they detected the five  $^{13}\text{C}$  isotopologues of  $\text{HC}_5\text{N}$ , they could not determine well their relative abundances due to low signal-to-noise ratios (3 – 6). Takano et al. (1998) also reported the spectra of the two  $^{13}\text{C}$  isotopologues,  $\text{HC}^{13}\text{CCCCN}$  and  $\text{HCCCC}^{13}\text{CN}$ , with slightly higher signal-to-noise ratios ( $\approx 8$ ). However, they could

not discuss its main formation pathway, because of the lack of data for the other three  $^{13}\text{C}$  isotopologues.

In the present paper, we observed the five  $^{13}\text{C}$  isotopologues of  $\text{HC}_5\text{N}$  toward TMC-1 CP with the NRO 45-m telescope with high enough signal-to-noise ratios to constrain mechanisms responsible for the formation of  $\text{HC}_5\text{N}$ .

## 2. Observations

We carried out observations of the normal species and the five  $^{13}\text{C}$  isotopologues of  $\text{HC}_5\text{N}$  with the NRO 45-m radio telescope in 2014 March, April (2013-2014 season), December, and 2015 January (2014-2015 season). The observed position was  $(\alpha_{2000}, \delta_{2000}) = (04^{\text{h}}41^{\text{m}}42^{\text{s}}.49, 25^{\circ}41'27''.0)$  for TMC-1 CP. The Z45 receiver (Nakamura et al. 2015) and the high electron mobility transistor (HEMT) amplifier receiver (H22), both of which can obtain dual-polarization data simultaneously, were used for the observations of the  $J = 16 - 15$  and  $J = 9 - 8$  transitions at 42 GHz and 23 GHz, respectively. The exact frequencies of the observed lines are given in Table 1. The system temperatures of the Z45 and the H22 receivers were from 100 to 130 K, and from 90 to 110 K, respectively. The beam sizes and the main beam efficiencies ( $\eta_B$ ) were  $37''$  and 0.72 for 42 GHz (Nakamura et al. 2015), and  $72''$  and 0.8 for 23 GHz. The telescope pointing was checked every 1.5 hours by observing the SiO maser line ( $J = 1-0$ ) from NML Tau and GL 5134, and the pointing error was less than  $3''$ . We used the SAM45 FX-type digital correlator in frequency settings whose bandwidths and resolutions are 125 MHz and 30.52 kHz, respectively, for observations at 42 GHz, and 63 MHz and 15.26 kHz, respectively, for those at 23 GHz. These frequency resolutions correspond to the velocity resolution of about  $0.2 \text{ km s}^{-1}$ . We employed the position-switching mode, where the off-source position was set to be  $+30'$  away in the right ascension. The smoothed bandpass calibration method (Yamaki et al. 2012) was adopted

in the analysis, which allows us to greatly improve the signal-to-noise ratios, compared with the standard position-switch observations. In fact, the scan pattern of this method was a set of 20 seconds and 5 seconds for on-source and off-source positions, respectively. We applied 60 and 32 channel-smoothing for the off-source spectra at 23 GHz and 42 GHz, respectively.

### 3. Results and Analysis

#### 3.1. Results

The spectra of the five  $^{13}\text{C}$  isotopologues of  $\text{HC}_5\text{N}$  were taken with signal-to-noise ratios of 12 – 20, as shown in Figures 1. We also obtained high quality data for the normal species. Since the spectra show a symmetric single peak structure, we fitted the spectra with a Gaussian profile, and obtained the spectral line parameters, as summarized in Table 1. The line widths ( $\Delta v$  [ $\text{km s}^{-1}$ ]) in the 23 GHz region ( $\sim 0.8 \text{ km s}^{-1}$ ) are broader than those in the 42 GHz region ( $\sim 0.5 \text{ km s}^{-1}$ ). Although the origin of their difference is unclear, the following possibility can be considered. It is well known that the TMC-1 CP region has a complex velocity structure (Langer et al. 1995; Dickens et al. 2001). Since the telescope beam samples a wider area at 23 GHz than at 42 GHz, the line width could be larger at 23 GHz. However, this difference does not affect our discussion on the relative abundance ratios among the five  $^{13}\text{C}$  isotopologues seriously, and hence, we do not discuss the line width further. The values of  $V_{\text{LSR}}$  are consistent with one another, and are in good agreement with the  $V_{\text{LSR}}$  value reported for this source ( $5.85 \text{ km s}^{-1}$ , Kaifu et al. (2004)).

The ratio of the integrated intensities ( $\int T_{\text{A}}^* dv$  [ $\text{K km s}^{-1}$ ]) of the five  $^{13}\text{C}$  isotopologues is derived to be 1.00 : 0.95 : 0.97 : 1.01 : 1.16 ( $\pm 0.16$ ) ( $1\sigma$ ) and 1.00 : 1.01 : 1.12 : 1.13 : 1.17 ( $\pm 0.19$ ) ( $1\sigma$ ) for  $[\text{H}^{13}\text{CCCCCN}]$  :  $[\text{HC}^{13}\text{CCCCN}]$  :  $[\text{HCC}^{13}\text{CCCN}]$  :  $[\text{HCCC}^{13}\text{CCN}]$  :

[HCCCC<sup>13</sup>CN] for the  $J = 9 - 8$  and  $J = 16 - 15$  lines, respectively. Although HCCCC<sup>13</sup>CN is slightly brighter than the other species, there are no significant differences in intensities among the five <sup>13</sup>C isotopologues. The result contrasts with that for HC<sub>3</sub>N, which shows clear differences in intensities of the three <sup>13</sup>C isotopologues (Takano et al. 1998).

### 3.2. Analysis

The rotational population of HC<sub>5</sub>N is not completely thermalized to the gas kinetic temperature, because the H<sub>2</sub> density of TMC-1 CP ( $4 \times 10^4 \text{ cm}^{-3}$  (Hirahara et al. 1992)) is equal to or lower than the critical densities of the HC<sub>5</sub>N lines. However, Takano et al. (1990) showed that the observed brightness temperatures of the HC<sub>5</sub>N lines are well approximated by the rotation temperature of 6.5 K. Then, we calculated the column densities of the normal species and the five <sup>13</sup>C isotopologues of HC<sub>5</sub>N using the local thermodynamic equilibrium (LTE) as shown the following formulae (Takano et al. 1998):

$$\tau = -\ln \left[ 1 - \frac{T_A^*}{f\eta_B \{J(T_{\text{ex}}) - J(T_{\text{bg}})\}} \right], \quad (1)$$

where

$$J(T) = \frac{h\nu}{k} \left\{ \exp\left(\frac{h\nu}{kT}\right) - 1 \right\}^{-1}, \quad (2)$$

and

$$N = \tau \frac{3h\Delta\nu}{8\pi^3} \sqrt{\frac{\pi}{4\ln 2}} Q \frac{1}{\mu^2} \frac{1}{J_{\text{lower}} + 1} \exp\left(\frac{E_{\text{lower}}}{kT_{\text{ex}}}\right) \left\{ 1 - \exp\left(-\frac{h\nu}{kT_{\text{ex}}}\right) \right\}^{-1}. \quad (3)$$

In equation (1),  $T_A^*$  denotes the antenna temperature,  $f$  the beam filling factor,  $\eta_B$  the main beam efficiency (see Section 2), and  $\tau$  the optical depth. We used 0.8 and 1 for  $f$  in the 23 GHz and 42 GHz band data, respectively. We employed these  $f$  values, because a size of the emitting region of carbon-chain molecules in TMC-1 CP is approximately 2.5' according to the mapping observations by Hirahara et al. (1992).  $T_{\text{ex}}$  is the excitation temperature,

$T_{\text{bg}}$  the cosmic microwave background temperature ( $\approx 2.7$  K), and  $J(T)$  in equation (2) the Planck function. We derived  $T_{\text{ex}}$  and  $\tau$  simultaneously from the observed intensities of the 23 GHz and 42 GHz lines by using the formula (1). In equation (3),  $N$  is the column density,  $\Delta v$  the line width (FWHM),  $Q$  the partition function,  $\mu$  the permanent electric dipole moment of  $\text{HC}_5\text{N}$  ( $4.33 \times 10^{-18}$  [esu cm](Alexander et al. 1976)), and  $E_{\text{lower}}$  the energy of the lower rotational energy level. In the energy level calculations, we used the rotational constants of the normal species and the  $^{13}\text{C}$  isotopologues (Alexander et al. 1976; Sanz et al. 2005).

The calculated column densities and the  $^{12}\text{C}/^{13}\text{C}$  ratios are summarized in Table 2. For the normal species, the excitation temperature and the column density are determined to be  $6.5 \pm 0.2$  K and  $(6.2 \pm 0.3) \times 10^{13} \text{ cm}^{-2}$ , respectively, where the errors are estimated from the Gaussian fits, and represent the confidence level of one standard deviation. The optical depths for the  $J = 9 - 8$  and  $16 - 15$  lines are  $1.084 \pm 0.014$  and  $1.19 \pm 0.03$  ( $1\sigma$ ), respectively. The obtained excitation temperature and column density of the normal species are consistent with the previous result ( $6.5 \pm 0.2$  K and  $(6.3 \pm 0.6) \times 10^{13} \text{ cm}^{-2}$ ) (Takano et al. 1990) within the error ranges.

We calculated the column densities of the five  $^{13}\text{C}$  isotopologues using equation (3) and the excitation temperature derived for the normal species (6.5 K). The calculated column densities of the normal species and the five  $^{13}\text{C}$  isotopologues, and the  $^{12}\text{C}/^{13}\text{C}$  ratios are summarized in Table 2. For the five  $^{13}\text{C}$  isotopologues, the column densities were derived to be  $(6.4 \pm 0.9) \times 10^{11}$ ,  $(6.2 \pm 0.8) \times 10^{11}$ ,  $(6.6 \pm 0.8) \times 10^{11}$ ,  $(6.7 \pm 0.9) \times 10^{11}$ , and  $(7.4 \pm 0.9) \times 10^{11} \text{ cm}^{-2}$ , for  $\text{H}^{13}\text{CCCCCN}$ ,  $\text{HC}^{13}\text{CCCCN}$ ,  $\text{HCC}^{13}\text{CCCN}$ ,  $\text{HCCC}^{13}\text{CCN}$ , and  $\text{HCCCC}^{13}\text{CN}$ , respectively. The abundance ratio of the  $^{13}\text{C}$  isotopologues of  $\text{HC}_5\text{N}$  is then  $1.00 : 0.97 : 1.03 : 1.05 : 1.16$  ( $\pm 0.19$ ) ( $1\sigma$ ) for  $[\text{H}^{13}\text{CCCCCN}] : [\text{HC}^{13}\text{CCCCN}] : [\text{HCC}^{13}\text{CCCN}] : [\text{HCCC}^{13}\text{CCN}] : [\text{HCCCC}^{13}\text{CN}]$ . This



result agrees with those obtained from integrated intensities. The averaged  $^{12}\text{C}/^{13}\text{C}$  ratio of  $\text{HC}_5\text{N}$  is  $94 \pm 6$  ( $1\sigma$ ), which is slightly higher than the elemental ratio of  $60 - 70$  in the local interstellar medium (e.g., Langer & Penzias 1990, 1993; Savage et al. 2002; Milam et al. 2005). The intensities are also affected by the calibration errors (main beam efficiency and filling factor). However, we obtained the data of the normal species and the five  $^{13}\text{C}$  isotopologues simultaneously. Then, these calibration errors do not affect the  $^{12}\text{C}/^{13}\text{C}$  ratios. We discuss these ratios in section 4.2.

We investigated the sensitivities of the assumed  $T_{\text{ex}}$  values on the column densities and the  $^{12}\text{C}/^{13}\text{C}$  ratios. We calculated the column densities of the normal species and the five  $^{13}\text{C}$  isotopologues using  $T_{\text{ex}}$  of 5.9 K and 7.1 K, which are the lowest and highest values in the  $3\sigma$  error range of the excitation temperature. We derived the column densities of the normal species to be  $(7.0 \pm 0.5) \times 10^{13} \text{ cm}^{-2}$  and  $(4.7 \pm 0.2) \times 10^{13} \text{ cm}^{-2}$  for 5.9 K and 7.1 K, respectively. The column densities of the  $^{13}\text{C}$  isotopologues were not significantly affected by the change of the excitation temperature. The  $^{12}\text{C}/^{13}\text{C}$  ratios averaged for the five isotopologues are  $125 \pm 6$  ( $1\sigma$ ) and  $89 \pm 5$  ( $1\sigma$ ) for 5.9 K and 7.1 K, respectively. Although the  $^{12}\text{C}/^{13}\text{C}$  ratios slightly depend on the excitation temperature, the  $^{12}\text{C}/^{13}\text{C}$  ratio of  $\text{HC}_5\text{N}$  is still higher than that of the elemental ratio in the local interstellar medium.

We also evaluated the ratio by using the excitation temperature derived for each  $^{13}\text{C}$  isotopologue. We derived  $T_{\text{ex}}$  to be  $6.2 \pm 0.6$ ,  $6.2 \pm 0.6$ ,  $6.3 \pm 0.5$ ,  $6.3 \pm 0.6$ , and  $6.3 \pm 0.5$  K ( $1\sigma$ ) for  $\text{H}^{13}\text{CCCCCN}$ ,  $\text{HC}^{13}\text{CCCCN}$ ,  $\text{HCC}^{13}\text{CCCN}$ ,  $\text{HCCC}^{13}\text{CCN}$ , and  $\text{HCCCC}^{13}\text{CN}$ , respectively, from the intensities of the observed two rotational transitions. These results are consistent with the value obtained from the normal species (6.5 K) within the errors, which implies that we can neglect the effect of self-trapping for the normal species. We then calculated the column densities using  $T_{\text{ex}}$  obtained for each  $^{13}\text{C}$  isotopologue. The  $^{13}\text{C}$  isotopic fractionation is not affected by the changes in  $T_{\text{ex}}$ , and the  $^{12}\text{C}/^{13}\text{C}$  ratios are also

not affected within the errors. The results are also shown in Table 2.

## 4. Discussion

### 4.1. Formation mechanisms of $\text{HC}_5\text{N}$

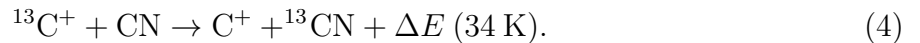
We here consider possible reactions leading to cyanopolyynes, using the UMIST Database for Astrochemistry 2012 (McElroy et al. 2013). By focusing on the rate constants, activation energies, abundances and formation pathways of precursors, we can sketch formation pathways of cyanopolyynes, as shown in Figure 2. Three types of formation pathways are possible as follows:

Pathway 1: the reactions of  $\text{C}_{2n}\text{H}_2 + \text{CN}$ ,

Pathway 2: the growth of the cyanopolyyne carbon chains via  $\text{C}_2\text{H}_2^+ + \text{HC}_{2n+1}\text{N}$ , and

Pathway 3: the reactions between hydrocarbon ions and nitrogen atoms followed by electron recombination reactions.

For  $\text{HC}_3\text{N}$ , Pathway 1 is suggested to play a dominant role in its production: Takano et al. (1998) reported that the main formation pathway of  $\text{HC}_3\text{N}$  is the reaction of  $\text{C}_2\text{H}_2 + \text{CN}$  on the basis of their observational results of  $^{13}\text{C}$  isotopic fractionation. Fractionation of  $^{13}\text{C}$  in CN proceeds through the following reaction (Kaiser et al. 1991):



This reaction is exothermic with energy of 34 K due to decreasing the zero-point vibrational energy. Hence, its backward reaction is not effective in cold dark clouds, where the typical temperature is approximately 10 K (e.g., Benson & Myers 1989). As a result, the  $^{12}\text{C}/^{13}\text{C}$  ratio for CN decreases in comparison with those for hydrocarbons such as  $\text{C}_2\text{H}_2$  and  $\text{C}_4\text{H}_2$ , because similar fractionation processes of  $^{13}\text{C}$  do not occur in hydrocarbons (Watson et al. 1976).

If  $\text{HC}_5\text{N}$  is mainly formed by Pathways 1 and/or 2, at least one carbon atom in  $\text{HC}_5\text{N}$ , possibly that adjacent to the nitrogen atom, is not equivalent to the others. Assuming that  $\text{HC}_5\text{N}$  is mainly formed by Pathway 2, the  $^{13}\text{C}$  isotopic fractionation of  $\text{HC}_5\text{N}$  should be  $x : y : 1.0 : 1.0 : 1.4$ , where  $x$  and  $y$  are arbitrary values, for  $[\text{H}^{13}\text{CCCCCN}] : [\text{HC}^{13}\text{CCCCN}] : [\text{HCC}^{13}\text{CCCN}] : [\text{HCCC}^{13}\text{CCN}] : [\text{HCCCC}^{13}\text{CN}]$ , unless scrambling of the carbon atoms is efficient. However, our observed abundances are roughly equal for all the  $^{13}\text{C}$  isotopologues. It is not likely that Pathway 1 and 2 are the main formation pathways of  $\text{HC}_5\text{N}$ .

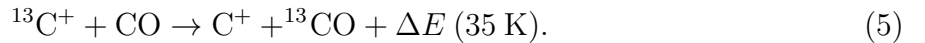
On the basis of the above consideration, we propose that Pathway 3 should significantly contribute to formation of  $\text{HC}_5\text{N}$ . In Pathway 3, all carbon atoms in  $\text{HC}_5\text{N}$  originate from the hydrocarbon ions. If all the carbon atoms in the mother hydrocarbon ion have the similar  $^{12}\text{C}/^{13}\text{C}$  ratio, the observational result can be explained. This seems indeed possible for a large hydrocarbon ion, because it is generally produced through various processes. This pathway is similar to the chemical model calculation by Markwick et al. (2000), where  $\text{HC}_5\text{N}$  can be produced through the reaction between a hydrocarbon ion ( $\text{C}_5\text{H}_3^+$ ) and a nitrogen atom. Thus, we propose that Pathway 3 overwhelms Pathways 1 and 2, resulting in almost equivalent abundances of the  $^{13}\text{C}$  isotopologues of  $\text{HC}_5\text{N}$ .

Based on the above discussion on  $\text{HC}_5\text{N}$ , we also propose that the longer cyanopolyynes may be formed by a mechanism similar to that of  $\text{HC}_5\text{N}$ , namely the reactions between hydrocarbon ions and nitrogen atoms. However, it is difficult to confirm our suggestion by observations of  $^{13}\text{C}$  isotopic fractionation at the present. Langston & Turner (2007) tentatively detected the  $^{13}\text{C}$  isotopologues of  $\text{HC}_7\text{N}$  using the  $J = 11 - 10$  and  $12 - 11$  transitions for the first time in the interstellar medium. They calculated the averaged  $^{12}\text{C}/^{13}\text{C}$  ratio of  $\text{HC}_7\text{N}$ , but they could not study its  $^{13}\text{C}$  isotopic fractionation as they only derived upper limits for each of the seven  $^{13}\text{C}$  isotopologues. Hence, more sensitive

observations are needed to confirm the flat  $^{13}\text{C}$  abundance over the seven  $^{13}\text{C}$  isotopologues of  $\text{HC}_7\text{N}$ . In the theoretical model by Markwick et al. (2000), the pathways leading to  $\text{HC}_7\text{N}$  and  $\text{HC}_9\text{N}$  via reactions between hydrocarbon ions ( $\text{C}_7\text{H}_3^+$  and  $\text{C}_9\text{H}_3^+$ , respectively) and nitrogen atoms followed by the electron recombination reactions are presented. The most interesting point to emerge from our analysis is that cyanopolyynes longer than  $\text{HC}_5\text{N}$  are mainly produced by the reactions between hydrocarbon ions and nitrogen atoms, whereas  $\text{HC}_3\text{N}$  is mainly produced by the neutral-neutral reaction between  $\text{C}_2\text{H}_2$  and  $\text{CN}$ . One possible reason is high abundance of  $\text{C}_2\text{H}_2$  (Markwick et al. 2000).

#### 4.2. Dilution of the $^{13}\text{C}$ species

We compile  $^{12}\text{C}/^{13}\text{C}$  ratios of some carbon-chain molecules at TMC-1 CP in Table 3. The  $^{12}\text{C}/^{13}\text{C}$  ratios of carbon-chain molecules show more or less higher than that of the local interstellar elemental ratio (60 – 70) (e.g., Langer & Penzias 1990, 1993; Savage et al. 2002; Milam et al. 2005). This can be explained by the following reaction, which should be effective under low-temperature conditions (e.g., Watson et al. 1976; Langer et al. 1984),



The reaction leads to a reduction in  $^{13}\text{C}^+$ . Consequently,  $^{13}\text{C}$  isotopologues of carbon-chain molecules are also reduced, because  $\text{C}^+$  and  $\text{C}$  are important raw materials of carbon-chain molecules.

We derived the five  $^{12}\text{C}/^{13}\text{C}$  ratios of  $\text{HC}_5\text{N}$ , and they are slightly higher than those of  $\text{HC}_3\text{N}$  (see Table 3). Langston & Turner (2007) were able to detect the  $^{13}\text{C}$  isotopologues only by combining the observations of all seven isotopologues of  $\text{HC}_7\text{N}$  into one spectrum. They derived the averaged  $^{12}\text{C}/^{13}\text{C}$  ratio of  $\text{HC}_7\text{N}$  by combination of multiple lines of the seven  $^{13}\text{C}$  isotopologues of  $\text{HC}_7\text{N}$ . These ratios indicate that the  $^{13}\text{C}$  species of the

cyanopolyynes are less diluted than other carbon-chain molecules. For example, for  $\text{HC}_3\text{N}$  and  $\text{HC}_5\text{N}$ , the  $^{12}\text{C}/^{13}\text{C}$  ratios coincide among their  $^{13}\text{C}$  isotopologues within about 20% and 10%, respectively. On the other hand, for CCS,  $^{12}\text{C}/^{13}\text{C}$  of  $^{13}\text{CCS}$  is about 4 times larger than that of  $\text{C}^{13}\text{CS}$ . In other words, an interesting characteristic of the  $^{12}\text{C}/^{13}\text{C}$  ratios of the two cyanopolyynes is that their differences appear to be small among the  $^{13}\text{C}$  isotopologues of each cyanopolyne, compared to other carbon-chain molecules. The reason why the  $^{13}\text{C}$  species of the cyanopolyynes are not significantly diluted is unclear. Mechanisms of the dilution of the  $^{13}\text{C}$  species are still controversial and are left for future studies.

## 5. Conclusions

We carried out observations of the  $J = 9 - 8$  and  $16 - 15$  rotational transitions of the normal species and the five  $^{13}\text{C}$  isotopologues of  $\text{HC}_5\text{N}$  toward TMC-1 CP with the NRO 45-m telescope. The abundance ratios of the five  $^{13}\text{C}$  isotopologues are found to be  $1.00 : 0.97 : 1.03 : 1.05 : 1.16$  ( $\pm 0.19$ ) ( $1\sigma$ ) for  $[\text{H}^{13}\text{CCCCCN}] : [\text{HC}^{13}\text{CCCCN}] : [\text{HCC}^{13}\text{CCCN}] : [\text{HCCC}^{13}\text{CCN}] : [\text{HCCCC}^{13}\text{CN}]$ . Based on the result, we suggest that reactions between hydrocarbon ions and nitrogen atoms play an important role in the formation of  $\text{HC}_5\text{N}$ . We derived the  $^{12}\text{C}/^{13}\text{C}$  ratios from the five  $^{13}\text{C}$  isotopologues of  $\text{HC}_5\text{N}$ . The averaged value is  $94 \pm 6$  ( $1\sigma$ ), and the  $^{13}\text{C}$  species of cyanopolyynes are less diluted than other carbon-chain molecules.

We are grateful to the staff of Nobeyama Radio Observatory. Nobeyama Radio Observatory is a branch of the National Astronomical Observatory of Japan, National Institutes of Natural Sciences. In particular, we deeply appreciate Mr. Jun Maekawa for developing a software for smoothed bandpass calibration analysis, and Dr. Izumi Mizuno for discussing the method of smoothed bandpass calibration analysis. We express

our thanks to Prof. Kazuhito Dobashi and Dr. Tomomi Shimoikura (Tokyo Gakugei University) for discussing analysis of the data obtained by using the Z45 receiver, and to all the Z45 receiver group members for their kind support. The Z45 receiver is supported in part by a Grant-in-Aid for Science Research of Japan (24244017) and the National Science Foundation under Grant (NSF PHY11-25915).

## REFERENCES

- Alexander, A. J., Kroto, H. W., & Walton, D. R. M. 1976, JMoSp, 62, 175
- Benson, P.J., & Myers, P. C. 1989, ApJS, 71, 89
- Dickens, J. E., Langer, W. D., & Velusamy, T. 2001, ApJ, 558, 693
- Fukuzawa, K., Osamura, Y., & Schaefer, H. F. 1998, ApJ, 505, 278
- Hirahara, Y., Suzuki, H., Yamamoto, S., et al. 1992, ApJ, 394, 539
- Kaifu, N., Ohishi, M., Kawaguchi, K., et al. 2004, PASJ, 56, 69
- Kaiser, M. E., Hawkins, I., & Wright, E. L. 1991, ApJ, 379, 267
- Langer, W. D., Graedel, T. E., Frerking, M. A., & Armentrout, P. B. 1984, ApJ, 277, 581
- Langer, W. D., & Penzias, A. A. 1990, ApJ, 357, 477
- Langer, W. D., & Penzias, A. A. 1993, ApJ, 408, 539
- Langer, W. D., Velusamy, T., Kuiper, T. B. H., et al. 1995, ApJ, 453, 293
- Langston, G., & Turner, B. 2007, ApJ, 658, 455
- Markwick, A. J., Millar, T. J., & Charnley, S. B. 2000, ApJ, 535, 256
- McElroy, D., Walsh, C., Markwick, A. J., et al. 2013, A&A, 550, A36
- Milam, S. N., Savage, C., Brewster, M. A., Ziurys, L. M., & Wyckoff, S. 2005, ApJ, 634, 1126
- Müller, H. S. P., Schlöder, F., Stutzki, J., & Winnewisser, G. 2005, JMoSt, 742, 215
- Nakamura, F., Ogawa, H., Yonekura, Y., et al. 2015, PASJ, in press (arXiv:1509.02631)

- Sakai, N., Ikeda, M., Morita, M., et al. 2007, *ApJ*, 663, 1174
- Sakai, N., Saruwatari, O., Sakai, T., Takano, S., & Yamamoto, S. 2010, *A&A*, 512, A31
- Sakai, N., Takano, S., Sakai, T., et al. 2013, *JPCA*, 117, 9831
- Sanz, M. E., McCarthy, M. C., & Thaddeus, P. 2005, *J. Chem. Phys.*, 122, 194319
- Savage, C., Apponi, A. J., Ziurys, L. M., & Wyckoff, S. 2002, *ApJ*, 578, 211
- Seki, K., Yagi, M., He, M., Halpern, J. B., & Okabe, H. 1996, *CPL*, 258, 657
- Sims, I. R., Queffelec, J. -L., Travers, D., et al. 1993, *CPL*, 211, 461
- Suzuki, H., Yamamoto, S., Ohishi, M., et al. 1992, *ApJ*, 392, 551
- Takano, S., Suzuki, H., Ohishi, M., et al. 1990, *ApJ*, 361, L15
- Takano, S., Masuda, A., Hirahara, Y., et al. 1998, *A&A*, 329, 1156
- Wakelam, V., Loison, J. -C., Herbst, E., et al. 2015, *ApJS*, 217, 20
- Watson, W. D., Anicich, V. G., & Huntress, Jr., W. T. 1976, *ApJ*, 205, L165
- Woon, D. E., & Herbst, E. 1997, *ApJ*, 477, 204
- Yamaki, H., Kamenno, S., Beppu, H., Mizuno, I., & Imai, H. 2012, *PASJ*, 64, 118
- Yoshida, K., Sakai, N., Tokudome, T., et al. 2015, *ApJ*, 807, 66



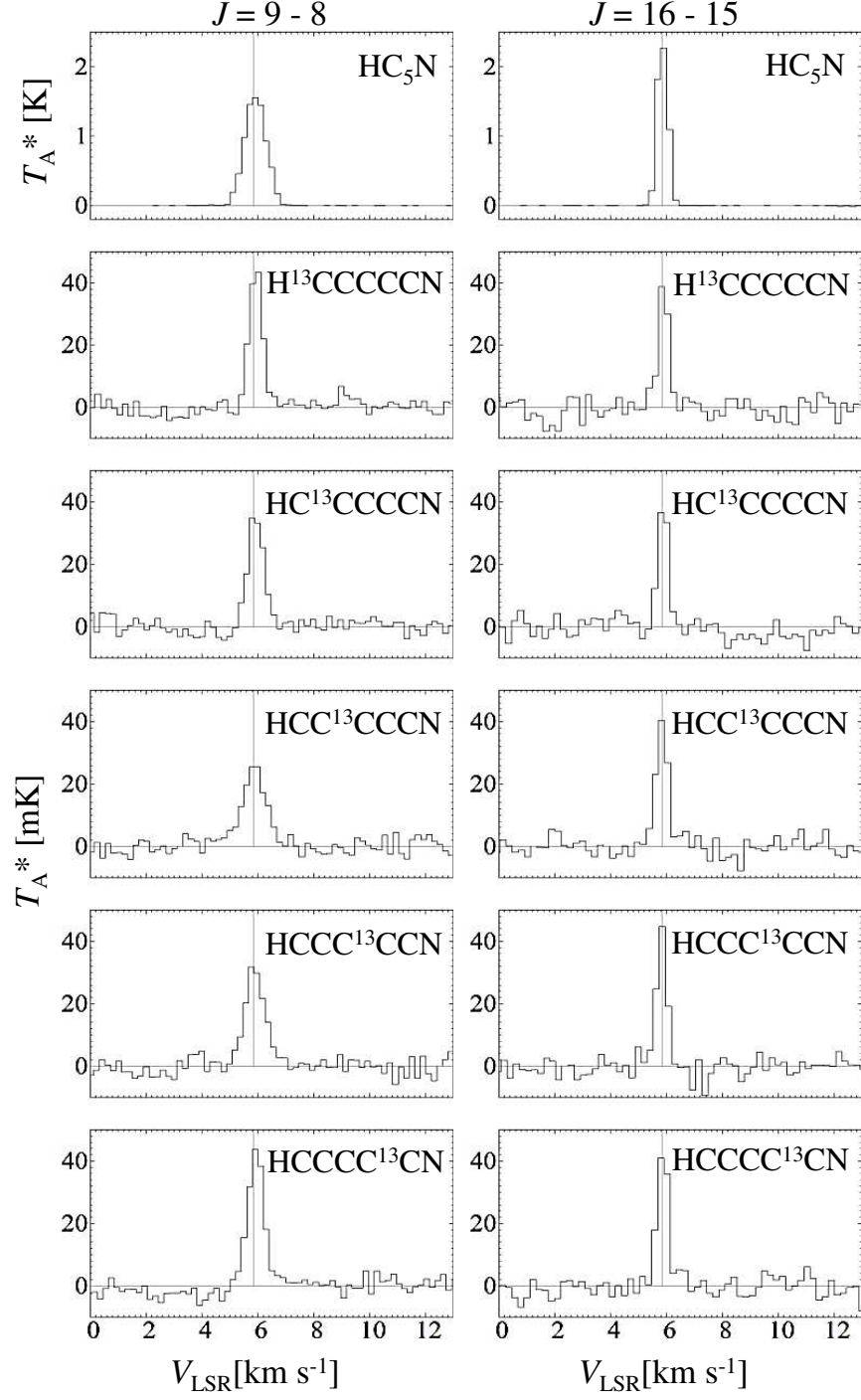


Fig. 1.— Spectra of  $\text{HC}_5\text{N}$  and its  $^{13}\text{C}$  isotopologues of the  $J = 9 - 8$  and  $16 - 15$  rotational transitions toward TMC-1 CP.  $\text{HC}^{13}\text{CCCCCN}$  and  $\text{HCCCC}^{13}\text{CN}$ ,  $\text{HCC}^{13}\text{CCCN}$  and  $\text{HCCC}^{13}\text{CCN}$  have been observed in the same IF bands. The vertical lines show  $V_{\text{LSR}} = 5.85 \text{ km s}^{-1}$ .

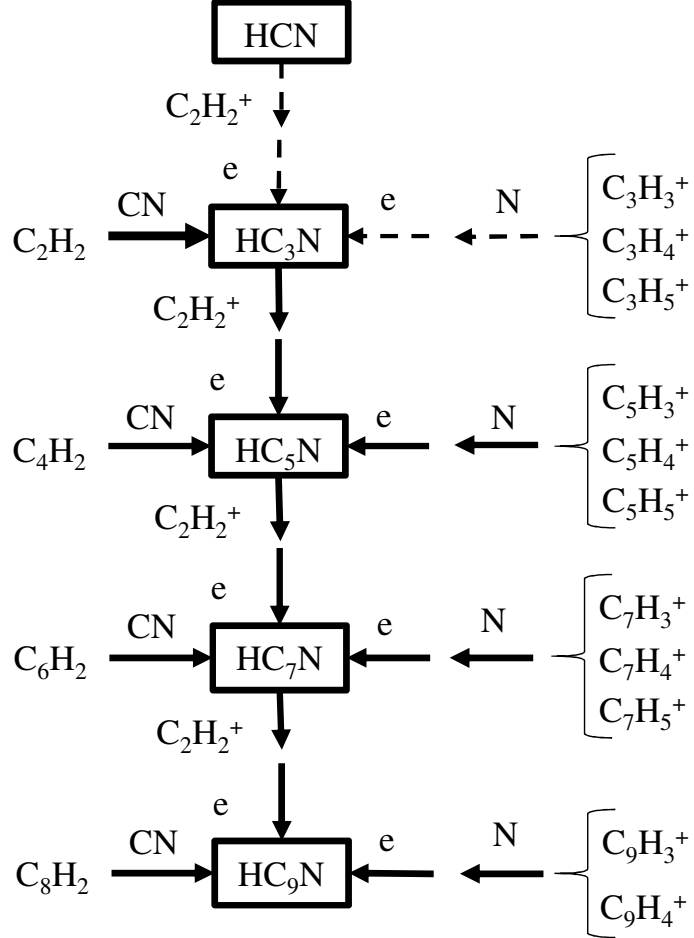


Fig. 2.— Formation pathways leading to cyanopolyynes. The heavy line and dotted lines show the main and less contributed pathways, respectively (Takano et al. 1998).

Table 1. Spectral line parameters of HC<sub>5</sub>N and its five <sup>13</sup>C isotopologues

Species	Transition	Frequency <sup>a</sup> [GHz]	$T_{\text{A}}^*$ <sup>b</sup> [mK]	$\Delta v$ [km s <sup>-1</sup> ]	$V_{\text{LSR}}$ [km s <sup>-1</sup> ]	$\int T_{\text{A}}^* dv^c$ [K km s <sup>-1</sup> ]	rms <sup>d</sup> [mK]
HC <sub>5</sub> N	9 – 8	23.9639007 (1)	1600 (20)	0.88 (1)	5.90 (9)	1.50 (3)	2.6
	16 – 15	42.6021529 (2)	1874 (57)	0.46 (2)	5.9 (2)	0.93 (4)	3.3
H <sup>13</sup> CCCCCN	9 – 8	23.3400887 (5)	44 (2)	0.57 (3)	6.0 (3)	0.027 (2)	2.2
	16 – 15	41.4931720 (9)	31 (3)	0.44 (4)	5.8 (5)	0.0147 (19)	3.2
HC <sup>13</sup> CCCCN	9 – 8	23.7183241 (5)	35 (2)	0.67 (4)	5.8 (3)	0.025 (2)	2.4
	16 – 15	42.1655778 (9)	31 (3)	0.44 (4)	5.8 (4)	0.0148 (16)	3.0
HCC <sup>13</sup> CCCN	9 – 8	23.9390819 (6)	25 (1)	0.97 (6)	5.8 (3)	0.026 (2)	2.1
	16 – 15	42.5580316 (9)	31 (3)	0.49 (4)	5.8 (4)	0.0165 (16)	3.1
HCCC <sup>13</sup> CCN	9 – 8	23.9419974 (5)	31 (2)	0.81 (5)	5.8 (3)	0.027 (2)	2.1
	16 – 15	42.5632150 (9)	35 (3)	0.45 (4)	5.9 (4)	0.0166 (19)	3.1
HCCCC <sup>13</sup> CN	9 – 8	23.7271659 (6)	43 (2)	0.69 (4)	5.9 (3)	0.031 (2)	2.4
	16 – 15	42.1812962 (10)	35 (3)	0.47 (4)	5.8 (5)	0.0172 (18)	3.0

Note. — The numbers in parenthesis represent one standard deviation in the Gaussian fit except for frequency.

<sup>a</sup>Taken from the Cologne Database for Molecular Spectroscopy (CDMS) (Müller et al. 2005).

<sup>b</sup>We calibrated the peak intensities of the  $J = 16 - 15$  rotational transitions. We divided the results of Gaussian fit by 1.3, which was obtained by comparing Suzuki et al. (1992) and Nakamura et al. (2015).

<sup>c</sup>We calculated the integrated intensities and their errors using  $T_{\text{A}}^*$  and  $\Delta v$ , which are determined by the Gaussian fit, where the errors are estimated from those of  $T_{\text{A}}^*$  and  $\Delta v$ .

<sup>d</sup>The rms noises in emission-free regions.

Table 2. Column densities and  $^{12}\text{C}/^{13}\text{C}$  ratios of  $\text{HC}_5\text{N}$

Species	Column Density <sup>a</sup> [ $\times 10^{11} \text{ cm}^{-2}$ ]	$^{12}\text{C}/^{13}\text{C}$ <sup>a</sup> ratio	Column Density <sup>b</sup> [ $\times 10^{11} \text{ cm}^{-2}$ ]	$^{12}\text{C}/^{13}\text{C}$ <sup>b</sup> ratio
$\text{HC}_5\text{N}$	$(6.2 \pm 0.3) \times 10^2$			
$\text{H}^{13}\text{CCCCCN}$	$6.4 \pm 0.9$	$98 \pm 14$	$7.0 \pm 1.0$	$89 \pm 13$
$\text{HC}^{13}\text{CCCCN}$	$6.2 \pm 0.8$	$101 \pm 14$	$6.8 \pm 0.9$	$91 \pm 12$
$\text{HCC}^{13}\text{CCCN}$	$6.6 \pm 0.8$	$95 \pm 12$	$6.8 \pm 0.9$	$91 \pm 12$
$\text{HCCC}^{13}\text{CCN}$	$6.7 \pm 0.9$	$93 \pm 13$	$6.9 \pm 1.0$	$90 \pm 13$
$\text{HCCCC}^{13}\text{CN}$	$7.4 \pm 0.9$	$85 \pm 11$	$7.5 \pm 1.0$	$83 \pm 11$

Note. — The error corresponds to one standard deviation.

<sup>a</sup>The values of  $^{13}\text{C}$  isotopologues were calculated by using  $T_{\text{ex}} = 6.5 \text{ K}$  obtained from the normal species.

<sup>b</sup>The values were calculated by using the  $T_{\text{ex}}$  derived for each isotopologue.

Table 3. The  $^{12}\text{C}/^{13}\text{C}$  ratios in various carbon-chain molecules toward TMC-1 CP

Species	$^{12}\text{C}/^{13}\text{C}$ ratio	Reference
$\text{HC}_3\text{N}/\text{H}^{13}\text{CCCN}$	$79 \pm 11$ ( $1\sigma$ )	1
$\text{HC}_3\text{N}/\text{HC}^{13}\text{CCN}$	$75 \pm 10$ ( $1\sigma$ )	1
$\text{HC}_3\text{N}/\text{HCC}^{13}\text{CN}$	$55 \pm 7$ ( $1\sigma$ )	1
$\text{HC}_5\text{N}/\text{H}^{13}\text{CCCCCN}$	$98 \pm 14$ ( $1\sigma$ )	2
$\text{HC}_5\text{N}/\text{HC}^{13}\text{CCCCN}$	$101 \pm 14$ ( $1\sigma$ )	2
$\text{HC}_5\text{N}/\text{HCC}^{13}\text{CCCN}$	$95 \pm 12$ ( $1\sigma$ )	2
$\text{HC}_5\text{N}/\text{HCCC}^{13}\text{CCN}$	$93 \pm 13$ ( $1\sigma$ )	2
$\text{HC}_5\text{N}/\text{HCCCC}^{13}\text{CN}$	$85 \pm 11$ ( $1\sigma$ )	2
$\text{HC}_7\text{N}/\text{average } ^{13}\text{C isotopologues}$	$87^{+35}_{-19}$ ( $1\sigma$ )	3
$\text{CCH}/^{13}\text{CCH}$	$>250$	4
$\text{CCH}/\text{C}^{13}\text{CH}$	$>170$	4
$\text{C}_4\text{H}/^{13}\text{CCCCH}$	$141 \pm 44$ ( $3\sigma$ )	5
$\text{C}_4\text{H}/\text{C}^{13}\text{CCCH}$	$97 \pm 27$ ( $3\sigma$ )	5
$\text{C}_4\text{H}/\text{CC}^{13}\text{CCH}$	$82 \pm 15$ ( $3\sigma$ )	5
$\text{C}_4\text{H}/\text{CCC}^{13}\text{CH}$	$118 \pm 23$ ( $3\sigma$ )	5
$\text{CCS}/^{13}\text{CCS}$	$230 \pm 130$ ( $3\sigma$ )	6
$\text{CCS}/\text{C}^{13}\text{CS}$	$54 \pm 5$ ( $3\sigma$ )	6
$\text{C}_3\text{S}/^{13}\text{CCCS}$	$>206$ ( $3\sigma$ )	5
$\text{C}_3\text{S}/\text{C}^{13}\text{CCS}$	$48 \pm 15$ ( $3\sigma$ )	5
$\text{C}_3\text{S}/\text{CC}^{13}\text{CS}$	30 - 206	5

References. — (1) Takano et al. 1998; (2) This work (3) Langston & Turner 2007; (4) Sakai et al. 2010; (5) Sakai et al. 2013; (6) Sakai et al. 2007.